ORGANIC LETTERS

2012
Vol. 14, No. 7
1788–1791

# Enhanced Photochemical [6$\pi$] Electrocyclization within the Lipophilic Protein Binding Site

**Mireia Marin, Virginie Lhiaubet-Vallet,* and Miguel A. Miranda***

*Instituto de Tecnología Química UPV-CSIC, Universidad Politecnica de Valencia, Avda de Los Naranjos s/n, 46022 Valencia, Spain*

*lvirgini@itq.upv.es; mmiranda@qim.upv.es*

**Received February 16, 2012**

## ABSTRACT

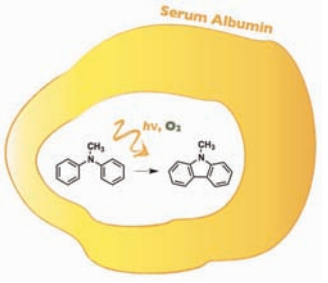


**Photocyclization of *N*-methyldiphenylamine to *N*-methylcarbazole is achieved within the microenvironment provided by site I of serum albumins. Quantum yield determinations, combined with transient absorption spectroscopic detection of the dihydrocarbazole intermediate, demonstrate that protein encapsulation provides a subtle control of the kinetic parameters, leading to optimized efficiencies.**

Photochemical [6$\pi$] electrocyclizations are well-established tools for the synthesis of a large variety of carbocyclic or heterocyclic compounds.[1] These reactions have also found application in fields such as actinometry,[2] photochromism,[3] or design of molecular devices.[4] From a mechanistic point of view, they typically arise from the first ($\pi$,$\pi$*) singlet excited state.[5] An interesting exception relies on the oxidative photocyclization of diarylamines (see Figure 1 for the case of *N*-methyldiphenylamine), which occurs through a multistep pathway involving two consecutive triplet excited states. Initial formation of 4a,4b-dihydrocarbazoles is followed by oxidation to carbazoles.[2a,6] Oxygen plays a dual role: on the one hand, it disfavors the reaction by quenching the amine triplet excited state, whereas on the other hand, it is required as a reagent for the final oxidative step.[7] In this context, the binding sites of serum albumins (SAs) would represent an ideal microenvironment to optimize the photocyclization efficiency by providing a subtle control of the involved kinetic parameters.

Upon encapsulation, the photobehavior of guest molecules is modulated not only as a result of conformational restrictions imposed by the rigidity of protein cavities, but also by the controlled diffusion of oxygen.[8] These two aspects have been previously tackled by comparing the kinetic parameters of *N*-methyldiphenylamine photocyclization in micro-heterogeneous media with those obtained in water.[9,10] In the case of cyclodextrins, a lower rate of

(1) (a) Bach, T.; Hehn, J. P. *Angew. Chem., Int. Ed.* **2011**, *50*, 1000. (b) Albini, A.; Fagnoni, M. In *Handbook of Synthetic Photochemistry*; Wiley-VCH: Weinheim, 2010.

(2) (a) Förster, E. W.; Grellmann, K.-H.; Linschitz, H. *J. Am. Chem. Soc.* **1973**, *95*, 3108. (b) Yoshihara, T.; Yamaji, M.; Itoh, T.; Nishimura, J.; Shizuka, H.; Tobita, S. *J. Photochem. Photobiol., A* **2001**, *140*, 7.

(3) (a) Fukumoto, S.; Nakashima, T.; Kawai, T. *Angew. Chem Int. Ed.* **2011**, *50*, 1565. (b) Irie, M. *Photochem. Photobiol. Sci.* **2010**, *9*, 1535.

(4) (a) Irie, M. *Chem. Rev.* **2000**, *100*, 1685. (b) Golovkova, T. A.; Kozlov, D. V.; Neckers, D. C. *J. Org. Chem.* **2005**, *70*, 5545.

(5) Turro, N. J.; Ramamurthy, V.; Scaiano, J. C. In *Modern Molecular Photochemistry of Organic Molecules*; University Science Books: Sausalito, California, 2010; pp 856.

(6) (a) Grellmann, K.-H.; Kühnle, W.; Weller, H.; Wolff, T. *J. Am. Chem. Soc.* **1981**, *103*, 6889. (b) Görner, H. *J. Phys. Chem. A* **2008**, *112*, 1245.

(7) Fischer, G.; Fischer, E.; Grellman, K. H.; Linschitz, H.; Temizer, A. *J. Am. Chem. Soc.* **1974**, *96*, 6267.

(8) (a) Alonso, R.; Jimenez, M. C.; Miranda, M. A. *Org. Lett.* **2011**, *13*, 3860. (b) Lhiaubet-Vallet, V.; Bosca, F.; Miranda, M. A. *J. Phys. Chem. B* **2007**, *111*, 423–431. (c) Lhiaubet-Vallet, V.; Sarabia, Z.; Bosca, F.; Miranda, M. A. *J. Am. Chem. Soc.* **2004**, *126*, 9538. (d) Vaya, I.; Bueno, C. J.; Jimenez, M. C.; Miranda, M. A. *ChemMedChem* **2006**, *1*, 1015.

10.1021/ol3003805 
**Published on Web 03/14/2012**

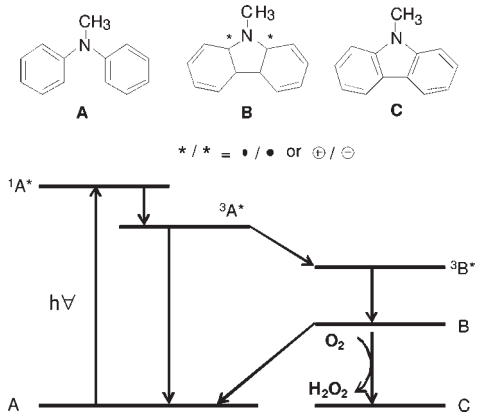


**Figure 1.** Structures of *N*-methyldiphenylamine (A), *N*-methyl-4a,4b-dihydrocarbazole (B), and *N*-methylcarbazole (C), together with an energetic diagram of the reaction mechanism.

photocyclization has been determined and attributed to restricted rotation inside the rigid oligosaccharide structure.[9] By contrast, no significant micellar effect has been found within SDS or CTAB vesicles.[10]

Here, it will be shown that the efficiency of *N*-methyldiphenylamine photocyclization is maximized within the microreactors provided by the lipophilic protein binding sites. This is achieved by exploiting the retarded intraprotein oxygen diffusion rate, which is markedly slower than amine triplet quenching in solution and faster than dihydrocarbazole dehydrogenation.

The reaction mechanism has been clearly established in previous works (Figure 1).[2a,6] After excitation and intersystem crossing (ISC), a short-lived triplet excited state ($^3$A*) is generated. It may return back to the ground state A in the submicrosecond time scale or undergo adiabatic ring closure, leading to the *N*-methyl-4a,4b-dihydrocarbazole triplet excited state ($^3$B*), which subsequently crosses to the corresponding ground state (B). In the presence of oxygen, dehydrogenation of B leads to the final product, namely, *N*-methylcarbazole (C). Conversely, under anaerobic conditions, B suffers an efficient ring-opening back to the starting material A (> 99% in non polar solvents).[2a,6b]

The reaction efficiency was determined through the photocyclization quantum yields. Experiments were performed both under air and oxygen, in acetonitrile or in buffered aqueous solution, in the presence or in the absence of SA. The overall study was performed with equimolar amounts of A and SA, in order to avoid multiple occupation of the protein binding site. Photoconversion of A to C was followed by UV−vis spectroscopy, as usually done for actinometry measurements. Formation of C was monitored by its characteristic absorption band peaking at 345 nm, which does not overlap with the reactant absorption spectrum.

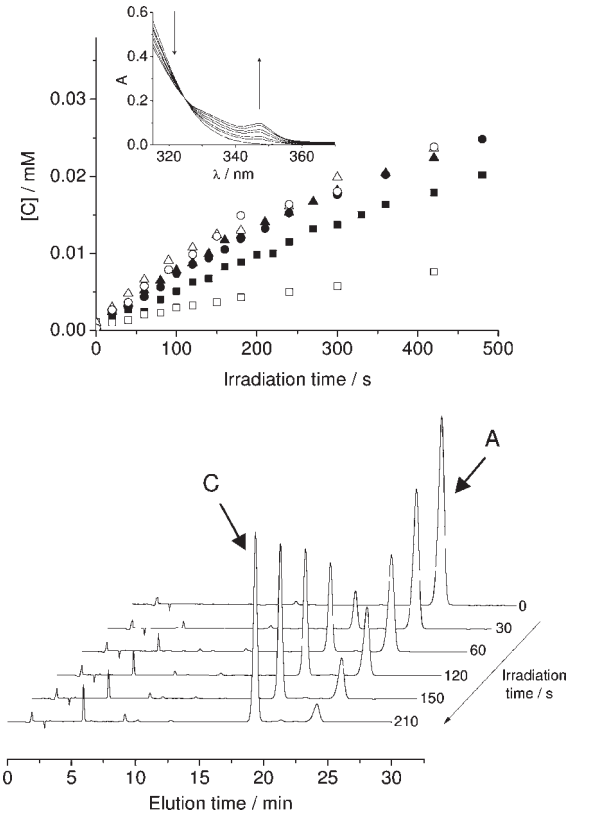


**Figure 2.** Top: concentration of carbazole C, determined from the absorbance changes monitored at 345 nm, plotted as a function of irradiation time for A ($8.25 \times 10^{-5}$ M) in MeCN (squares), PBS/HSA (triangles), and PBS/BSA (circles) under air (solid symbols) or oxygen (open symbols). Inset: UV spectral changes upon irradiation of an aerated PBS solution of A in the presence of HSA (molar ratio 1/1), during 323 nm monochromatic irradiation (from 0 to 30 min). Initial absorption spectrum of HSA was subtracted. Bottom: HPLC traces obtained during irradiation ($\lambda$ = 300 nm) of A ($1.65 \times 10^{-4}$ M) in aqueous buffer, in the presence of equimolar amounts of HSA.

Moreover, an isosbestic point at 323 nm was observed, as expected for a clean process (Figure 2 top, inset). This was confirmed by HPLC measurements, where C was detected as the only significant photoproduct both in solution and in protein media (Figure 2 bottom). Thus, the absorbance changes at 345 nm were plotted as a function of the irradiation time (Figure 2 top), and the quantum yields ($\phi_C$) were evaluated by the established procedure using A in aerated acetonitrile as standard (Table 1).[6b] An alternative determination of $\phi_C$ was also performed by steady state fluorescence, monitoring the increase of the C emission band ($\lambda_{max}$ = 367 nm) during irradiation of nonfluorescent A. As shown in Table 1, the data obtained with both methods were substantially coincident. It is highly remarkable that the value of $\phi_C$ increased largely in the presence of SAs, from 1.4- up to 4.6-fold. Interestingly, the highest $\phi_C$, obtained for BSA/$O_2$

(9) (a) Sur, D.; Purkayastha, P; Chattopadhyay, N. *J. Photochem. Photobiol., A* **2000**, *134*, 17. (b) Sur, D.; Purkayastha, P.; Chattopadhyay, N.; Bera, S. C. *J. Mol. Liq.* **2000**, *89*, 175.

(10) Roessler, N.; Wolff, T. *Photochem. Photobiol.* **1980**, *31*, 547.

system, was of 0.84. This is probably an upper limit, imposed by the intersystem crossing of the starting amine, which is the bottleneck and has been reported to occur with a $\phi_{ISC} = 0.8-0.9$ in solution.

**Table 1.** Photocyclization Quantum Yields Determined by UV−Vis Absorption and (In Parentheses) Steady State Fluorescence

| | PBS/MeCN[a] | MeCN | PBS/HSA | PBS/BSA |
|---|---|---|---|---|
| $\phi_C$(air) | 0.46 (0.44) | 0.45 (0.45)[b] | 0.63 (0.61) | 0.65 (0.67) |
| $\phi_C(O_2)$ | 0.55 (0.52) | 0.18 (0.19) | 0.73 (0.72) | 0.83 (0.84) |

[a] A 3/1 ratio was used to ensure complete dissolution of A and C. [b] Taken as standard value from ref 6b.

A satisfactory understanding of the influence of SAs on the photocylization was obtained from the study of the reaction intermediates. In this context, formation and decay of dihydrocarbazole B turned out to be a good reporter on the involved processes. This ground state species was safely characterized by laser flash photolysis (LFP), where it displayed a transient absorption band peaking at 610 nm.

Nanosecond LFP was performed at 308 nm with an excimer Xe/Cl laser, using PBS solutions of A ($4.1 \times 10^{-5}$ M) alone or in the presence of SAs ($4.1 \times 10^{-5}$ M). Under aerobic conditions, the transient absorption spectrum exhibited a weak maximum at 440 nm that decreased concomitantly with the increase of the much stronger band centered at 610 nm (Figure 3, top). By comparison with the literature, these species were assigned to $^3$B* and B, respectively.[2a,6b]

Interestingly, in bulk solution (aerated PBS), the decay at 610 nm followed a first order exponential law (eq 1) with a lifetime of 15 $\mu$s, whereas in the presence of SAs, a more complex fitting was required. The presence of two lifetime components ($\tau_f = 15\,\mu$s and $\tau_b = 451\,\mu$s for HSA, or $\tau_f = 15\,\mu$s and $\tau_b = 384\,\mu$s for BSA) was established by regression analysis of the decay curves according to eq 2. This observation is clearly associated with the location of the substrate in two different environments. The value of 15 $\mu$s, obtained for the shorter lifetime, corresponds to free intermediate B in bulk solution, while the longer-lived component reflects a tight interaction with one of the two well-established SA binding cavities, namely, site I or site II.[11] In this context, an analogous treatment of the decays for several [HSA]/[A] ratios was performed to obtain $a_f$ and $a_b$ preexponential factors (see eq 2), necessary to estimate the percentage of the substrate in each environment. As shown at the bottom of Figure 3, in the presence of equimolar amounts of HSA, ca. 90% of the substrate is complexed within the protein. A similar behavior was observed for BSA.

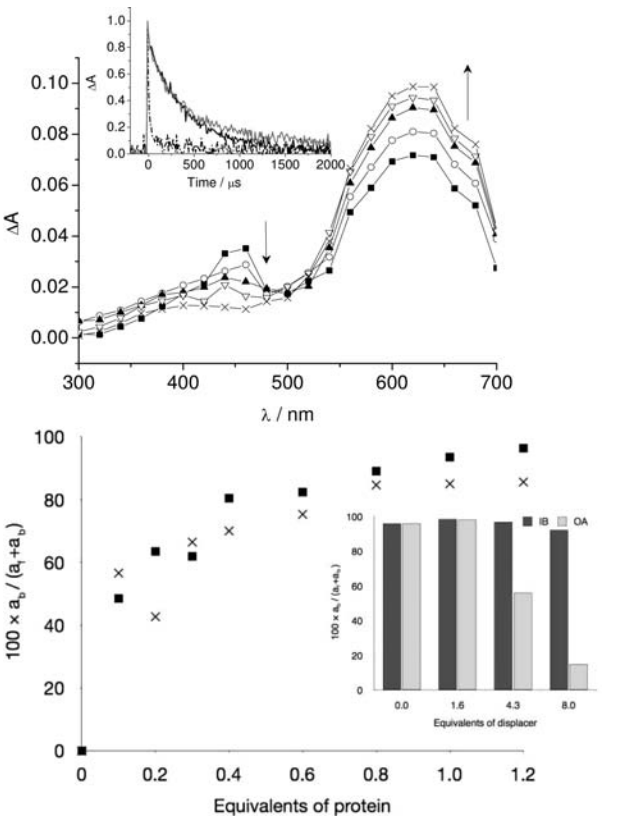


**Figure 3.** Top: transient absorption spectra of an aerated solution of A in aqueous buffer, in the presence of HSA ($4.1 \times 10^{-5}$ M, molar ratio 1/1) obtained from 0.4 to 4 $\mu$s after the 308 nm laser pulse. Inset: normalized decays monitored at 610 nm for A alone in PBS (dotted line) or in the presence of HSA (black line) or BSA (gray line). Bottom: percentage of protein-complexed substrate, as a function of the number of protein equivalents [SA]/[A] for HSA (closed squares) and BSA (crosses). Inset: percentage of the complexed substrate in the presence of equimolar amounts of HSA, as a function of added displacer concentration (IB = (*S*)-ibuprofen, OA = oleic acid).

$$\Delta A = \Delta A_0 + a_f \times e^{-t/\tau_f} \quad (1)$$

$$\Delta A = \Delta A_0 + a_f \times e^{-t/\tau_f} + a_b \times e^{-t/\tau_b} \quad (2)$$

Next, site assignment was achieved using oleic acid (OA) and (*S*)-ibuprofen (IB) as specific displacement probes for site I and site II, respectively.[12] For this purpose, increasing amounts of OA were added to aerated solutions of A/HSA (molar ratio 1/1), and transient decays were monitored at 610 nm. This led to a decrease of the long-lived component, $a_b$, concomitantly with an increase of the free A fraction, $a_f$ (Figure 3 bottom, inset). By contrast, no significant changes were observed when IB was used as displacer. Similar results were obtained for BSA (see the Supporting Information). Overall, the above observations clearly

(11) (a) Sudlow, G.; Birkett, D. J.; Wade, D. N. *Mol. Pharmacol.* **1975**, *11*, 824. (b) Sudlow, G.; Birkett, D. J.; Wade, D. N. *Mol. Pharmacol.* **1976**, *12*, 1052.

(12) Montanaro, S.; Lhiaubet-Vallet, V.; Jimenez, M. C.; Blanca, M.; Miranda, M. A. *ChemMedChem* **2009**, *4*, 1196.

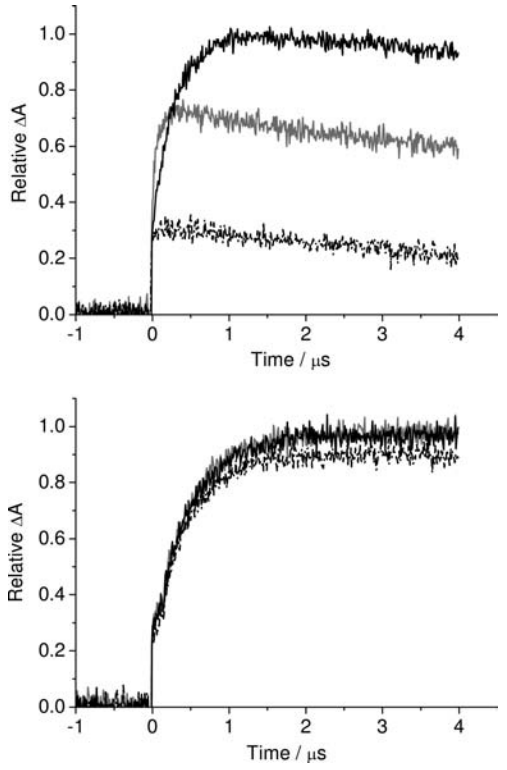


**Figure 4.** Top: transient absorption growths (monitored at 610 nm) of argon (black line), air (gray line), and oxygen (dotted line) bubbled solutions of A ($5.5 \times 10^{-5}$ M) in MeCN. Bottom: parallel experiment in aqueous buffer, in the presence of HSA ($5.5 \times 10^{-5}$ M).

demonstrate that substrate–protein interaction mainly occurs at the more hydrophobic binding site I of SAs.

In addition, transient absorption at 610 nm ($\Delta$A) corresponds to B intermediate and can be taken as an indicator of the efficiency of the cyclization process. For optically matched MeCN solutions, a clear difference was observed between oxygen, air, and argon bubbled solutions (Figure 4 top); formation of B was dramatically disfavored under aerated conditions because of the quenching of $^3$A* by oxygen. By contrast, in SA/PBS media, an oxygen independent growth was observed (Figure 4 bottom), as anticipated from the fast decay of $^3$A* compared to intraprotein diffusion of oxygen. The rate constant for quenching of the 610 nm absorbing species by oxygen within the protein was estimated to be $5.0 \times 10^5$ $M^{-1}$ $s^{-1}$ in HSA and $8.6 \times 10^5$ $M^{-1}$ $s^{-1}$ in BSA (assuming an intraprotein oxygen concentration similar to that reported for water). This value is ca. 2 orders of magnitude lower than oxygen diffusion within protein binding site I, which explains why the final dehydrogenation to carbazole C is not affected by complexation.[6b]

In summary, serum albumins provide an appropriate environment for optimization of diarylamine photocyclization. This is achieved by a subtle modulation of the kinetic parameters, as a result of the geometrical restrictions imposed by the protein cavities and the controlled diffusion of oxygen.

**Acknowledgment.** This work was funded by the Spanish Government (Project CTQ2009-13699, Ramon y Cajal contract RyC-2007-00476 to V.L.-V. and JAE-predoc contract to M.M.) and the Generalitat Valenciana (Prometeo/2008/090).

**Supporting Information Available.** Experimental procedures, displacement experiments and 610 nm transient absorption growth for A within BSA. This material is available free of charge via the Internet at http://pubs.acs.org.

The authors declare no competing financial interest.